Emission characteristics of CO, NO$_x$, SO$_2$ and indications of biomass burning observed at a rural site in eastern China

T. Wang, T. F. Cheung, and Y. S. Li

Department of Civil and Structural Engineering, Hong Kong Polytechnic University, Hong Kong, China

X. M. Yu

Linan Baseline Air Pollution Monitoring Station, Zhejiang, China

D. R. Blake

Department of Chemistry, University of California, Irvine, California, USA

[1] Atmospheric O$_3$, CO, SO$_2$, and NO$_y^*$ (NO$_y^* \approx$ NO + NO$_2$ + PAN + organic nitrates + HNO$_3$ + N$_2$O$_5$ + ...) were measured in 1999–2000 at a rural/agricultural site in the Yangtze Delta of China. In this paper we analyze the measurement results to show the emission characteristics of the measured gases and to infer relevant emission ratios. Positive correlations were found between CO and NO$_y^*$ with a slope (Δ[CO]/Δ[NO$_y^*$]) of 36 (ppbv/ppbv) for the winter and nighttime measurements. The ratio is considerably larger than that ($\approx$10 ppbv/ppbv) observed in the industrialized countries. The highest CO/NO$_y^*$ ratio (30–40 ppbv/ppbv) occurred in September–December 1999 and June 2000. The good correlation between CO and the biomass burning tracer CH$_3$Cl and the lack of correlation with the industrial tracer C$_2$Cl$_4$ suggests that the burning of biofuels and crop residues is a major source for the elevated CO and possibly for other trace gases as well. The average SO$_2$ to NO$_y^*$ ratio was 1.37 ppbv/ppbv, resulting from the use of relatively high-sulfur coals in China. The measured SO$_2$/NO$_y^*$ and ΔCO/ΔNO$_y^*$ were compared with the respective ratios from the current emission inventories for the study region, which indicated a comparable SO$_2$/NO$_x$ emission ratio but a large discrepancy for CO/NO$_x$. The observed CO to NO$_y^*$ ratio was more than 3 times the emission ratio derived from the inventories, indicating the need for further improvement of emission estimates for the rural/agricultural regions in China. Additional research will be needed to study the implications of rural emissions to atmospheric chemistry and climate on both regional and global scales. *INDEX TERMS:* 0365 Atmospheric Composition and Structure: Troposphere—composition and chemistry; 0345 Atmospheric Composition and Structure: Pollution—urban and regional (0305); 0394 Atmospheric Composition and Structure: Instruments and techniques; *KEYWORDS:* emission ratios, trace gases, NMHC, Yangtze Delta, rural China

1. Introduction

[2] In the past two decades, China has experienced phenomenal urban and industrial development. The increasing consumption of fossil fuels has led to an increasing emissions of major air pollutants, such as sulfur dioxide (SO$_2$), oxides of nitrogen (NO$_x$), and carbon monoxide (CO) [*Galloway*, 1989; *Kato and Akimoto*, 1994; *Streets and Waldhoff*, 2000]. The large emission of air pollutants has not only adversely affected air quality in major cities but has also caused pollution to occur on regional scales. The emission of SO$_2$ from coal burning has led to the formation of acid deposition over a large region in southern China [*Wang and Wang*, 1995]. The increasing emission of NO$_x$ and other ozone precursors have caused rural ozone concen-

trations high enough to depress China's winter wheat production [*Chameides et al.*, 1999a]. Atmospheric aerosols and pollution haze have been suggested to significantly reduce solar irradiance reaching the Earth's surface, which could in turn cause 5–30% reduction in the yields of rice and winter wheat in China [*Chameides et al.*, 1999b]. On a larger scale the massive expansions of China's vehicle fleet and road infrastructure has been suggested to have the potential to influence the tropospheric chemistry and the biogeochemical cycles in the remote Pacific Ocean [*Elliott et al.*, 1997].

[3] Rural areas of eastern China have some unique characteristics relevant to atmospheric environment studies. Approximately 80% of the nation's population reside in the rural/agricultural regions. The energy use pattern (and thus the emission characteristics) in rural regions can be rather different from urban areas. For example, biofuel is a main energy source for cooking and space heating in rural homes in China (as well as in other developing countries in Asia)

Figure 1.   Location of the study site.

[*Streets and Waldhoff*, 1998]. Additionally, with the industrial expansion the number of small factories has grown at a fast pace in many traditionally rural areas. Thus human activities and the resulting emissions in these areas (particularly in the populated coastal regions) can be quite significant. It is important to quantify concentrations of key trace gases and aerosols in the rural atmosphere in order to assess the level of exposure to pollution for the large rural population and to study environmental impacts of rural emissions. Atmospheric data in rural areas are also needed for elucidating atmospheric processes, reconciling emission inventories, and constraining chemical transport models. So far, field measurements outside urban centers in China have been very limited, especially those maintained for extended periods of time. The first large-scale field study of ozone (O_3) and related gases was carried out in 1994–1995 at several rural sites in eastern China [*Peng et al.*, 1997; *Luo et al.*, 2000]. In 1999 a field campaign took place in the Yangtze Delta region, during which we measured O_3, CO, SO_2, and NO_y^* from June 1999 to November 2000 at a typical rural/agricultural site. In addition, whole air samples were collected in 2-L stainless steel canisters and analyzed for organic compounds. The field study was part of a larger Chinese research program that was a cooperative effort with the China-MAP Project (the Yangtze Delta of China as an Evolving Metro-Agro-Plex). The overall seasonal variations of the measured gases and the ozone relationships with NO_y^* and CO have been shown by *Wang et al.* [2001a]. This present paper focuses on the emission patterns of CO, NO_x, and SO_2 observed at this rural site. The organic data are analyzed to suggest source(s) of elevated trace gases. The inferred emission ratios from the measurements are then compared with those derived from recently compiled inventories for the study region.

2.   Experiment

[4]   The study was conducted at the Linan Baseline Air Pollution Monitoring Station (30°25′N, 119°44′E, 132 m) in Zhejiang Province (Figure 1). The station is 53 km west and 210 km southwest of the major population centers of Hangzhou and Shanghai, respectively, with the Linan township (population: ∼50,000) 10 km to the south. To the west and farther south are sparsely populated and less developed mountainous regions. The measurement site is surrounded by hills planted in pines, mixed deciduous trees, and bamboo, as well as crop fields of various sizes in the valleys between the hills. Small villages are scattered around the station within a distance of a few kilometers. This land use pattern is typical in the rural part of eastern China.

[5]   Measurement instruments were housed in a laboratory situated on a hilltop. The laboratory had an air conditioner; however, the indoor temperature was not always controlled at a fixed level. Ambient air samples were drawn through a perfluoroalkoxy (PFA) Teflon tube (outside diameter, 12.7 mm; inside diameter, 9.6 mm; length, 8.5 m), which was connected to a PFA manifold. The inlet of the sample line was located 5 m above the rooftop of the laboratory. A bypass pump drew air at a rate of 15 L/min. With four analyzers the residence time of sampled air in the tube and the manifold was less than 2 s. An inline Teflon filter (Fluoroware Inc., Chaska, Minnesota) was placed upstream of each analyzer to prevent particles from entering into the analyzer.

[6]   The analyzers for measuring O_3, SO_2, and NO_y^* had been previously used in field studies at a coastal site in Hong Kong [*Wang et al.*, 1997, 2001b].

[7] O_3 was measured using a commercial UV photometric instrument (Thermo Environmental Instruments, Inc. (TEI), model 49) that had a detection limit of 2 ppbv and a 2-sigma (2-σ) precision of 2 ppbv for a 2-min average.

[8] SO_2 was measured by a pulsed UV fluorescence (TEI, model 43S), with a detection limit of 0.06 ppbv and 2-σ precision of 3% for ambient levels of 10 ppbv (2-min average). The uncertainty was estimated to be ∼9%. This estimate, however, does not include the possible additional errors caused by the loss of SO_2 in the unheated sampling line and by the interference of atmospheric water vapor [*Luke*, 1997].

[9]   CO was measured with a gas filter correlation, nondispersive infrared analyzer (Advanced Pollution Instrumentation, Inc., model 300) with a heated catalytic scrubber (as purchase) to convert CO to carbon dioxide (CO_2) for baseline determination. Our tests showed that nearly 100% of the water vapor was able to pass through the converter, although it could take a few minutes for the signal to reach an equilibrium. In our study, zeroing was conducted every 2 hours, each lasting 12 min. The 2-min data at the end of each zeroing were taken as the baseline and were automatically subtracted from the instrument signals. The detection limit was 30 ppbv for a 2-min average. The 2-σ precision was ∼1% for a level of 500 ppbv (2-min average) and the overall uncertainty was estimated to be 10%. The in situ CO data were compared with those from the analyses of 16 canister samples that were taken between 26 October and 2 November 1999 at the site and analyzed at the University of California, Irvine using the gas chromatographic method. (The concentrations of methane, $C_2–C_{10}$ nonmethane hydrocarbon (NMHCs) and $C_1–C_2$ halocarbon in the canister samples were also determined using a combination of gas chromatography with flame ionization detector

Table 1. Monthly Mean Mixing Ratios of CO, SO$_2$, NO$_y^*$, O$_3$ and Their Standard Deviations[a]

Month	CO, ppbv Daytime[b]	CO, ppbv Nighttime	SO$_2$, ppbv Daytime	SO$_2$, ppbv Nighttime	NO$_y^*$, ppbv Daytime	NO$_y^*$, ppbv Nighttime	O$_3$, ppbv Daytime	O$_3$, ppbv Nighttime	O$_3$, ppbv 1-hour Maximum
Aug. 1999	421 (170)	440 (155)	6.3 (4.7)	11.8 (10.0)	4.90 (2.5)	6.3 (2.5)	40 (16)	23 (12)	107
Sept. 1999	430 (214)	471 (196)	7.8 (6.7)	12.4(10.5)	6.0 (3.2)	7.7 (3.3)	46 (24)	25 (16)	136
Oct. 1999	661 (323)	669 (287)	10.8 (9.1)	13.5 (10.3)	10.0 (4.2)	10.6 (3.7)	44 (19)	29 (12)	112
Nov. 1999	740 (396)	787 (370)	17.1 (13.8)	22.6 (14.9)	11.6 (6.4)	12.8 (7.5)	40 (17)	26 (13)	87
Dec. 1999	734 (724)	802 (554)	22.5 (14.9)	26.7 (13.1)	17.1 (15.6)	18.7 (10.8)	40 (13)	27(10)	68
Jan. 2000	790 (475)	827 (484)	15.5 (11.4)	18.3 (16.3)	16.9 (11.4)	17.5 (11.1)	25 (15)	20 (13)	65
Feb. 2000	647 (219)	680 (251)	9.6 (6.4)	8.8 (7.0)	11.4 (5.4)	11.1 (6.6)	33 (13)	25 (15)	71
March 2000	614 (232)	674 (332)	11.7 (8.7)	17.2 (14.4)	12.2 (5.0)	12.7 (5.5)	41 (16)	29 (13)	76
April 2000	561 (206)	628 (240)	11.8 (10.1)	18.7 (14.5)	10.8 (4.3)	12.6 (5.0)	47 (18)	31(13)	83
May 2000	557 (260)	617 (228)	10.1 (8.5)	16.8 (11.4)	10.0 (3.9)	12.5 (4.1)	58 (23)	35 (17)	124
June 2000	383 (226)	433 (236)	8.3 (7.2)	13.8 (10.7)	7.9 (3.6)	9.2 (4.4)	46 (19)	28 (16)	118
July 2000	328 (192)	358 (155)	7.2 (5.9)	13.3 (10.1)	6.6 (3.2)	8.7 (3.1)	40 (19)	20 (14)	145

[a] Maximum 1-hour O$_3$ values in each month are also shown.
[b] Daytime, 0800-1959 LT; nighttime, 2000-0759 LT.

(GC/FID) and gas chromatography with electron capture detector and mass spectrometric detector (GC/ECD/MSD) techniques [*Blake et al.*, 1996].) The two sets of CO data correlate very well in the observed range of 350–1065 ppbv ([CO]$_{in\ situ}$ = 0.92[CO]$_{canister}$ + 20; r^2 = 0.97). The in situ concentrations were slightly lower than the canister results.

[10] NO was detected with a chemiluminescence analyzer (TEI, model 42S) with a detection limit of 0.05 ppbv. The 2-σ precision of this instrument was 4% (for NO = 10 ppbv) and the uncertainty was ∼10%. NO$_2$ was converted to NO using hot molybdenum oxide maintained to 325°C with the NO subsequently measured by the chemiluminescence detector. This technique is known to convert other reactive nitrogen species such as peroxyacetyl nitrate (PAN), aerosol nitrates (NO$_3^-$) and nitric acid (HNO$_3$). Thus the measured quantity approximates total reactive nitrogen, or NO$_y$ (where NO$_y$ = NO + NO$_2$ + PAN + HNO$_3$ + NO$_{3-}$ + N$_2$O$_5$ + HONO + organic nitrates + ...). In our experiment, NO$_{3-}$ was most likely being collected on the inline Teflon filter (which was replaced normally every 10 days). Most of HNO$_3$ was believed to have passed through the PFA sample line [*Neuman et al.*, 1999] during the short residence time, though some could be absorbed on the sample line and/or by aerosols collected on the filter. Our measurement using this conversion technique is hereafter referred to as NO$_y^*$. (We used the term "NO$_x^*$" for this measurement in our previous work [*Wang et al.*, 2001a].)

[11] The analyzers were checked every 5 hours (9 hours after April 2000) by injecting scrubbed ambient air (TEI, model 111) and a span gas mixture. A National Institute of Standards and Technology (NIST) traceable standard (Scott-Marrin Inc., California) containing 100.5 ppmv CO (±2%), 11.28 ppmv SO$_2$ (±5%), and 11.28 ppmv NO (±5%) was diluted using a custom-made calibrator with two mass flow controllers (Tylan General Inc., Torrance, California). The span and zero air were introduced to the analyzers through the inline particulate filter to account for possible losses of measured gases during normal measurement cycles. The O$_3$ analyzer was spanned using an internal ozonator inside the analyzer. Multipoint calibrations were performed at ∼3-month intervals by our personnel making the journey to the site. Local observatory staff carried out daily inspection of the instruments and replaced the inline filters. The automatic zero/span tests and data acquisition were conducted using a data logger (Environmental Systems Corporation, model 8816). One-minute averaged data were stored in the data logger and hourly averaged values are presented in this paper.

3. Results and Discussion

3.1. Overall Statistics

[12] Table 1 shows monthly averaged concentrations of CO, SO$_2$, NO$_y^*$, O$_3$, and their standard deviations. The statistics are calculated for daytime (0800–1959 LT) and nighttime (2000–0759 LT) periods. Also shown are maximum 1-hour O$_3$ concentrations in each month. Seasonal patterns are obvious for all these gases, with highest levels in winter for the primary pollutants and in late spring for ozone. The levels of primary pollutants are ∼1–5 times of those observed in rural areas in North America and Western Europe [e.g., *Parrish et al.*, 1991; *Parrish et al.*, 1993; *Buhr et al.*, 1995]. The observed winter peaks are believed to be
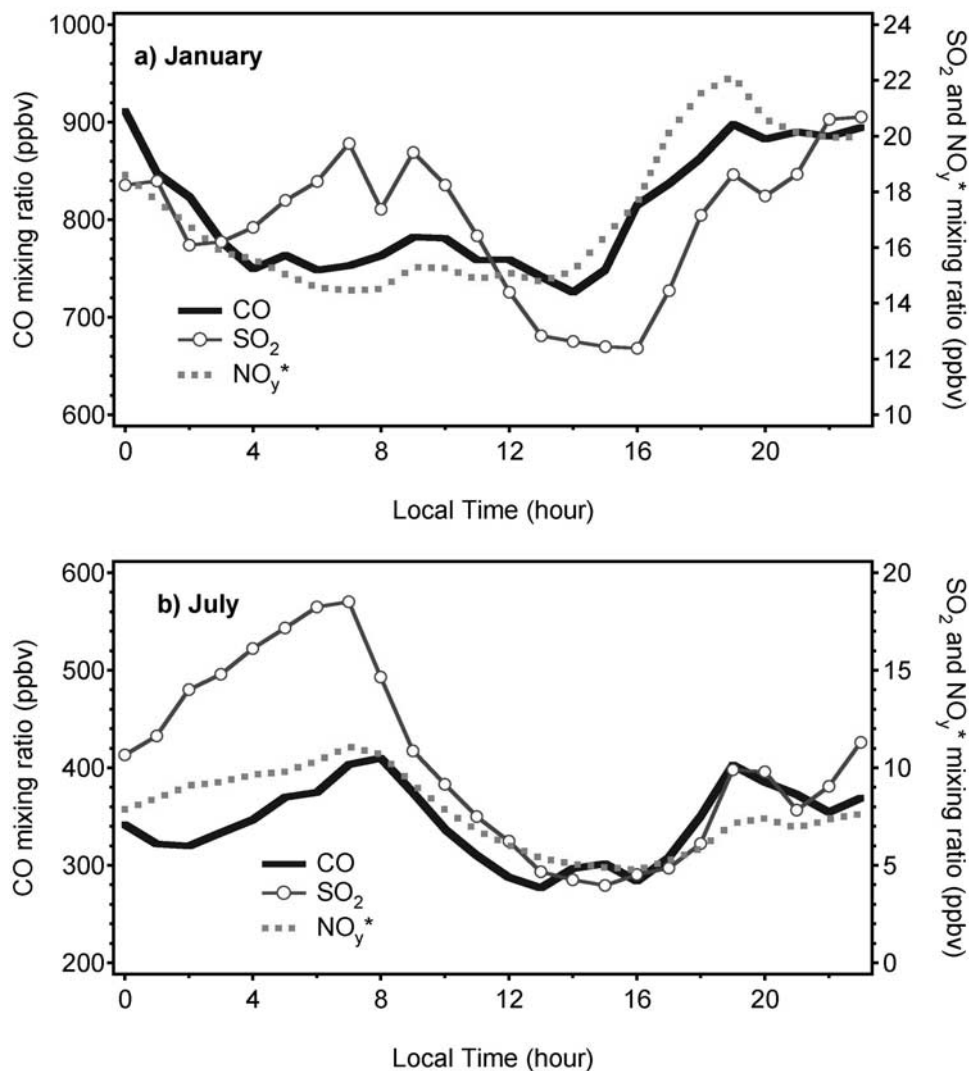
Figure 2. Diurnal cycles of CO, SO_2, and NO_y^* for (a) January and (b) July 2000.

due to weaker vertical mixing, slower chemical destruction, and probably a higher-energy demand (for heating) in winter. Low summertime values may be attributed to the rainy and unstable weather (with heaviest rainfall occurring in June) and also to the inflow of clean oceanic air brought in by the summer monsoon. Analysis of surface wind data from this site indicated that the winds were frequently from SSW with low speeds at night but changed to NNE during daytime with increasing speeds. This diurnal wind change appeared to be a result of the mountain valley flow induced by surface heating and the hilly topography of the study region.

[13] Figure 2 shows averaged diurnal cycles of the primary pollutants in winter (January 2000) and summer (July 2000). In general, higher levels of these gases were found at night than during daytime (the opposite is true for ozone, figure not shown.) The diurnal behaviors of these gases reflect the combined effects of diurnal changes in surface emissions, atmospheric transport (convection and advection), chemical transformation, and deposition processes, plus a compressed boundary layer at night. In winter

when temperature and solar radiation is low, chemical reactions slow down, and emission and dynamic transport processes are expected to have a bigger influence on the diurnal variations of the gases. The average CO mixing ratio in January was $\sim$900 ppbv at night with a lower value ($\sim$750 ppbv) between 0400 and 1600 LT. NO_y^* showed a similar diurnal variation with a nighttime value of $\sim$20 ppbv versus a daytime level of $\sim$15 ppbv, whereas SO_2 had an additional peak in the morning. The reduced levels of CO and NO_y^* in the 0400–1600 LT time window could be attributed to a smaller emission (e.g., reduced home heating) in the above period and/or increased daytime dilution by stronger winds and thicker boundary layer. In July, CO, SO_2, and NO_y^* levels were highest between 0600–0800 LT (e.g., [CO] $\approx$ 400 ppbv; [NO_y^*] $\approx$10 ppbv) and lowest between 1200–1600 LT (e.g., [CO] $\approx$ 280 ppbv; [NO_y^*] $\approx$ 5 ppbv). The elevated nighttime levels indicate an accumulation in the shallow nocturnal inversion layer of pollutants advected to the site from the adjacent rural areas. The rapid decreasing in daytime levels may be attributed to the
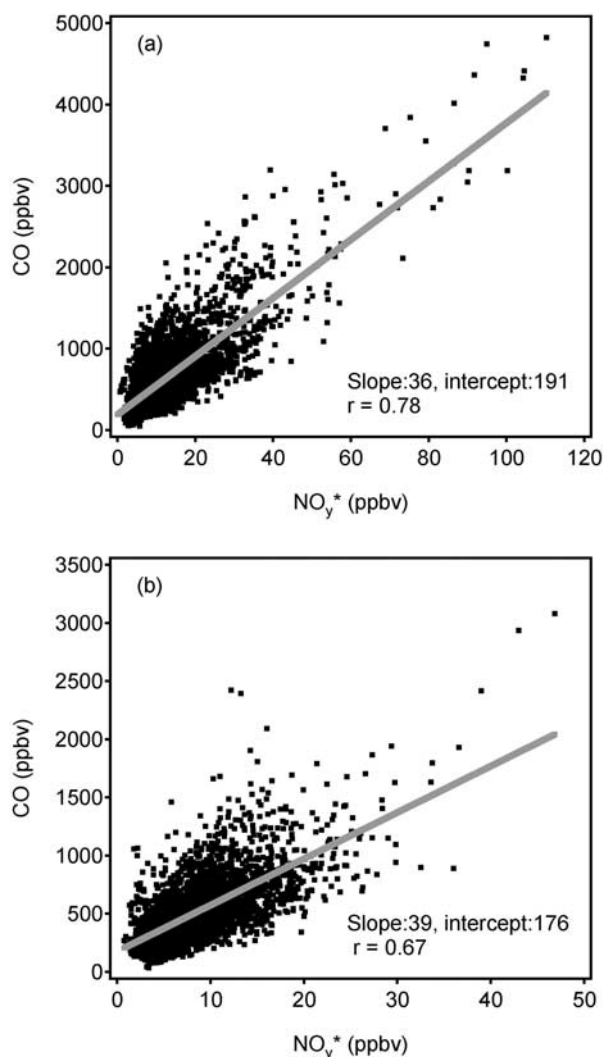
Figure 3. Correlation plots of CO-NO_y^* for (a) nighttime (2000–0759 LT) and all (24-hour) data in winter months (December, January, and February) and (b) daytime (0800–1959 LT) in nonwinter month.
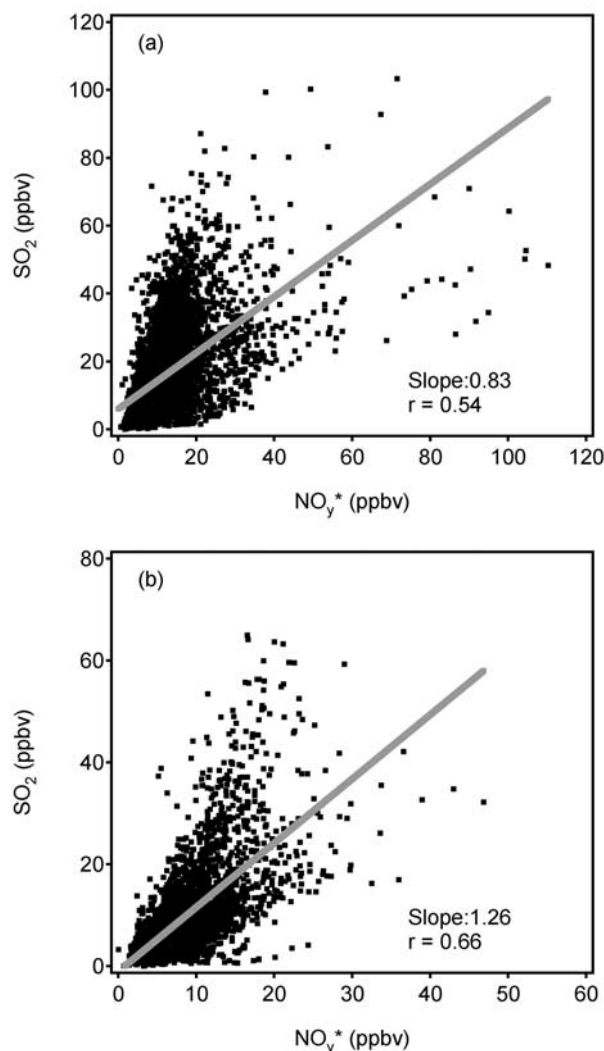
maximum values, and they estimated the emission ratios at a rural Alabama site. In the discussion below we will mainly report on the nighttime/winter data but will also compare with the results from the daytime data set.

3.2. Correlation of CO, NO_y^*, and SO_2

[15] Emission ratios can be inferred from the correlation of relevant compounds. Figure 3 shows the CO-NO_y^* scatterplots for both nighttime/winter and daytime data sets. In both data sets, CO and NO_y^* are reasonably well correlated, with a slope ($\Delta[CO]/\Delta[NO_y^*]$) of 36 and 39 ppbv/ppbv for the nighttime and daytime subsets, respectively. The intercept in the correlation plot can be interpreted as the background CO concentration for the study region, which is 176 and 191 ppbv for the two data sets, respectively. These values are higher than those ($\sim$120 ppbv) from the rural United States [*Parrish et al.*, 1991]. For SO_2 and NO_y^* (Figure 4) the data points are more scattered and tend to fall

dilution effect of the convective mixed layer in hot summer and the photochemical decay of NO_x (followed by the removal of HNO_3 and aerosol nitrate) and SO_2. It is interesting to note that SO_2 and NO_y^* showed a larger relative morning-afternoon decrease than CO, with SO_2 exhibiting the largest drop (from 18 to 4 ppbv). As a result, a lower SO_2 to NO_y^* ratio was found during daytime. A similar phenomenon was also observed in winter.

[14] To further examine the emission characteristics, we segregated the data into two groups. One contains measurements at nighttime (2000–0759 LT) plus all 24 hours in the three winter months (December, January, February); the other has only daytime (0800–1959 LT) values for nonwinter months. Since the nighttime/winter subset contains higher levels of pollutants and is also less affected by photochemical conversions of NO_x and SO_2, it should give the clearest signature of rural emissions for the study area. Similarly, *Buhr et al.* [1995] made use of data collected between 0000 and 0800, when several trace gases were at

Figure 4. Correlation plots of SO_2-NO_y^* for (a) nighttime (2000–0759 LT) and all (24-hour) data in winter months (December, January, and February) and (b) daytime (0800–1959 LT) in nonwinter month.
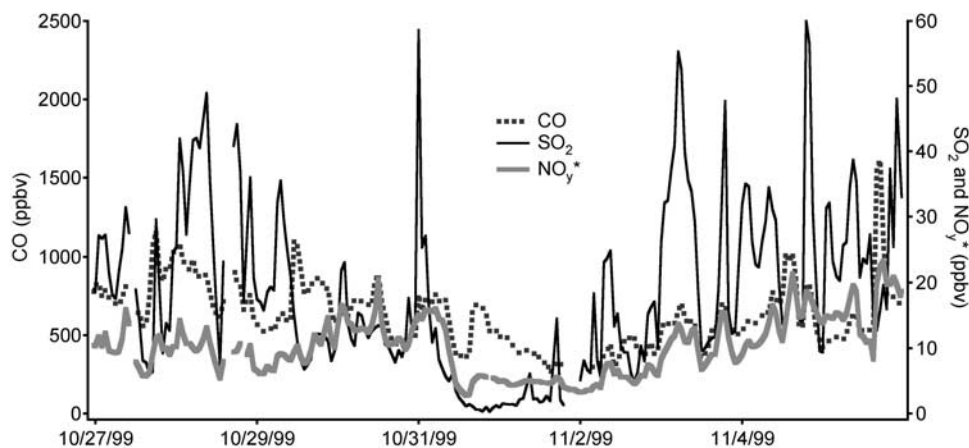
Figure 5. Time series of the concentrations of CO, SO_2, and NO_y^* between 27 October and 5 November 1999.

into two groups: one with higher SO_2 to NO_y^* ratios and one with lower ratios. The high SO_2/NO_y is characteristic of the emission from coal burning (e.g., in power generation plants), while low SO_2/NO_y is normally attributed to urban vehicle emissions [*Parrish et al.*, 1991].

[16] We further segregated the data into high-SO_2 ($SO_2/NO_y^* \geq 1$ ppbv/ppbv) and low-SO_2 ($SO_2/NO_y^* < 1$ ppbv/ppbv) subgroups and examined the CO-NO_y^* correlations in the two subsets. Interestingly, there was no significant difference in the slope between the high- and low-SO_2 cases. (The slopes were 32 and 37 ppbv/ppbv for high- and low-SO_2, respectively.) This result suggests that the CO and NO_y^* observed at Linan were emitted from a common source(s) that did not appear to emit significant amounts of SO_2. Inspection of the time series plots indicates that there were many occasions when SO_2 exhibited sharp peaks but CO and NO_y^* levels did not show large (or proportionally large) enhancements. Figure 5 gives examples of such cases, indicating a larger variability in SO_2 than in NO_y^*

and CO. The large variation of SO_2 is also reflected in the large standard deviations (relative to the means) in the monthly statistics (Table 1).

[17] We also examined the CO-NO_y^* correlation plots for each month in order to see whether the slope (and emission ratio) varied significantly with each season (see Figure 6). Both daytime and nighttime CO-NO_y^* slopes are shown in Figure 6 as well as the corresponding correlation coefficients (*r*). Several interesting features are worth mentioning. First, the slope is largest (daytime = 45–50 ppbv/ppbv; nighttime = 30–40, ppbv/ppbv) in September–December 1999 and June 2000, with lowest values ($\sim$20–25 ppbv/ppbv) in February and two summer months: July and August. The seasonal pattern is smoother in the daytime data set. The overall CO-NO_y^* relationship is dominated by the winter data (with a slope similar to that of the overall data set). Second, a diurnal difference is noticed. The daytime slopes are larger in most of the warm months, which is what one would expect because of the daytime
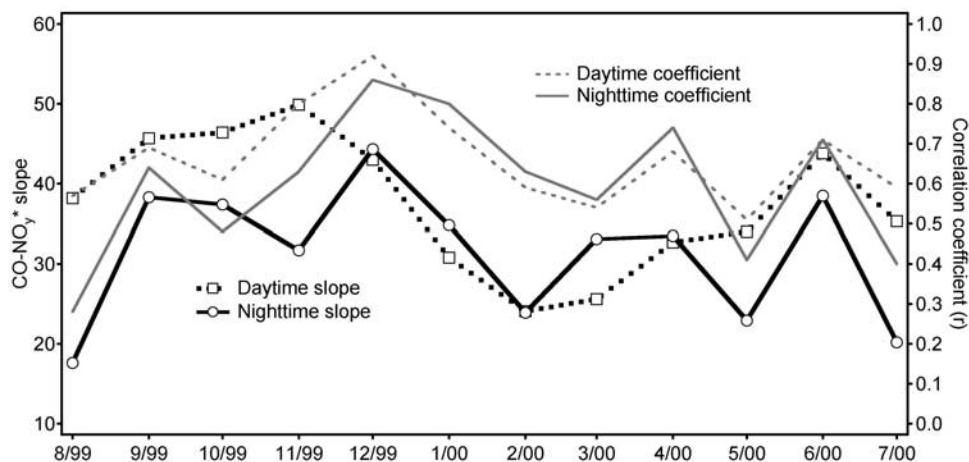
Figure 6. CO-NO_y^* slopes and correlation coefficients as a function of month.

Table 2. Averaged Mixing Ratios and Standard Deviations of Methane and C_2-C_{10} Nonmethane Hydrocarbons[a]

Species	Mean Mixing Ratio	Standard Deviation
Methane	1.922	0.046
Ethane	3351	927
Ethene	3068	1311
Ethyne	2603	880
Propane	1592	601
Propene	545	291
Propadiene	28	15
Propyne	57	29
1-Butene	97	48
n-Butane	593	287
i-Butane	494	216
2-Butene	10	11
2-mpentane	194	115
3-mpentane	168	86
Toluene	2544	1654
Benzene	1331	483
m+p-Xylene	323	193
Ethyl	193	112
o-Xylene	108	62
1,2,4-Trimethylbenzene	51	34
1,3,5-Trimethylbenzene	9	10
Isoprene	113	72
α-Pinene	59	28
2,2,4-Trimethylpentane	16	15
Octane	46	35
Cyclohexane	38	26
Nonane	33	23
Decane	28	20
Limonene	23	10

[a] All units are pptv except for methane which has a unit of ppmv. $N = 16$.

conversion of NO_x to HNO_3 followed by the removal (via wet and dry deposition) of HNO_3 from the air parcel. In contrast, in the three winter months (December, January, and February), the CO-NO_y^* slopes are very similar for daytime and nighttime data sets. This is also expected because of the slower rate of conversion of NO_x under lower temperatures and reduced sunlight in winter. Third, the wintertime CO-NO_y^* has the strongest correlation (with highest r), while data for other months show a larger degree of scattering. The above result appears to suggest that the sources that emit high CO (relative to NO_y) were strongest in September–December 1999 and June 2000. Examination of the monthly CO-SO_2 slopes (figure not shown) yielded a similar conclusion. Namely, higher CO-SO_2 slopes were found in September–December 1999, and a moderately large slope was indicated in June 2000. It is interesting to note that these high CO periods seem to follow the harvest of summer rice in October and winter wheat in late May in the study region.

[18] The CO/NO_x emission ratio derived from the present work is high compared to the results of previous studies conducted elsewhere. For example, based on the measurement of CO and NO_y, *Parrish et al.* [1991] found an emission ratio of ∼10 ppbv/ppbv for the Denver-Boulder area and a smaller ratio of 4−7 ppbv/ppbv for Scotia in rural Pennsylvania. In plumes emitted from urban Hong Kong, CO/NO_y was ∼3 ppbv/ppbv [*Kok et al.*, 1997]. (The very low CO/NO_y in Hong Kong is attributed to a large fleet of diesel vehicles). The much higher CO/NO_y^* (36 ppbv) at the Linan site suggests that very different combustion processes are responsible for the CO observed in the study area. We will examine this topic in more detail in the following section.

3.3. Relation of CO to NMHC

[19] To help explain the source(s) of elevated CO observed at this rural site, we examined methane, C_2-C_{10} NMHCs and C_1-C_2 halocarbon data. This information was based on the analyses of 16 whole air samples collected at the site between 26 October and 2 November 1999. (Note
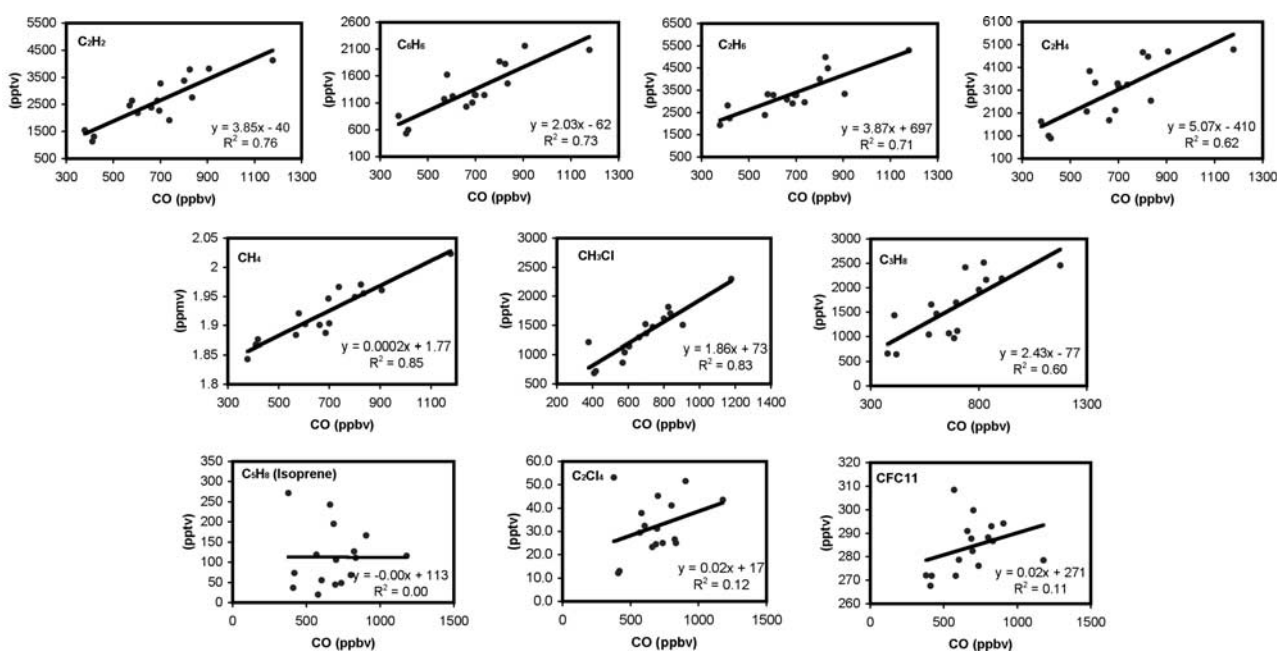
Figure 7. Correlation of CO with methane, several nonmethane hydrocarbons and halocarbons.

Table 3. Emission Ratios Derived From the Inventories and Measurements

	SO_2/NO_x	CO/NO_x
Zhejiang	1.12	11
Shanghai	1.07	11
Jiangsu	1.58	14
Jiangxi	2.08	22
Fuji	0.96	18
Measurement inferred[a]	1.37	36

[a] Based on the winter/nighttime data set.

that the sampling period happened to be in the months of high CO-NO$_y^*$ ratios.) Table 2 gives the mean mixing ratios and standard deviations of identified NMHCs. Figure 7 shows the correlations of CO with several NMHCs and halocarbons.

[20] Some interesting features can be seen in the NMHC data. The levels of ethane (mean = 3351 pptv) and propane (mean = 1592 pptv) are comparable to those found in rural areas of Europe and North America [e.g., *Colbeck and Harrison*, 1985; *Hov et al.*, 1991]. However, the levels of ethene, ethyne, benzene, and toluene are significantly enhanced at the Chinese site. Vehicular exhaust has long been known to be the major source of these compounds in urban areas [*Warneck*, 1988]. However, a closer examination of these data suggests that vehicle emissions are not the dominant source of these gases for this study site. One piece of evidence is that compounds released from vehicular fuel evaporation, such as butanes and pentanes, are not significantly elevated. Examination of the correlation plots provides further insight about the source of CO and the combustion-related NMHCs. Figure 7 shows that CO is positively correlated with methane ($r^2 = 0.85$), Methyl chloride ($r^2 = 0.83$), benzene ($r^2 = 0.73$), ethane ($r^2 = 0.71$), ethyne ($r^2 = 0.62$), ethene ($r^2 = 0.76$) but has little correlation with C_2Cl_4 and CFC-11. (As expected, CO is poorly correlated with biogenically emitted isoprene.) Methane and methyl chloride are emitted during biomass burning [*Lobert et al.*, 1991; *Blake et al.*, 1996] but have no significant source from vehicular exhaust. C_2Cl_4 has been considered a typical urban/industrial tracer [*Wang et al.*, 1995]. The lack of correlation between CO and C_2Cl_4 suggests that urban emissions (dominated by vehicular exhaust) are not the major source for CO (and probably also for ethene, ethyne, and benzene) observed at this rural site. Instead, the strong correlation of CO with CH_4 and CH_3Cl suggests a significant contribution from the burning of biomass such as biofuels and crop residues. This source attribution is supported by the fact that burning of fuel wood is very common for cooking food in the villages of the surrounding area and that burning crop residues (wheat in late May and rice in autumn) was frequently observed during our maintenance visits to the study site.

[21] It is of interest to compare the NMHC data from Linan with those obtained during the Pacific Exploratory-Mission West (PEM-West) studies [*Hoell et al.*, 1996, 1997]. Our data, though limited in sample number and time span, provide useful insights into the source signature for coastal eastern China. As one would expect, the levels of

the gases at our inland site are higher than in the Asian outflow air mass sampled over the Pacific Ocean. For example, the mean mixing ratio of ethane at Linan was 3351 pptv, compared to 2337 pptv determined in fresh Asian continental plumes with less than two days transport time and below 2-km altitude during PEM-West B in spring 1994 [*Blake et al.*, 1997; *Talbot et al.*, 1997]. For the shorter-lived benzene the difference is larger, 1331 pptv at Linan versus 180 pptv over the Pacific, which can be explained by the photochemical decay of benzene and the dilution effect as Asian plumes travel to the downwind regions over the Pacific. The magnitudes of ethyne/CO and propane/ethane have been used to indicate photochemical age of an air parcel [e.g., *Talbot et al.*, 1997]. At the Linan site, averaged ethyne/CO and propane/ethane are 3.8 pptv/ppbv and 0.47 pptv/pptv, respectively, which are similar to those (4.4 pptv/ppbv and 0.40 pptv/pptv) found in the low-altitude, fresh Asian continental plumes [*Talbot et al.*, 1997]. It is also interesting to note that the SO_2 to NO_y ratio over the western Pacific (1.13 ppbv/ppbv) found in the work of *Talbot et al.* [1997] was comparable to the emission ratio (1.37 ppbv/ppbv) derived from the Linan site.

3.4. Comparison With Emission Inventory

[22] *Streets and Waldhoff* [2000] compiled China's province-based emissions of NO_x, SO_2, and CO for 1995. Their updated estimates for year 2000 are given in the Web site: http://www.cgrer.uiowa.edu/people/carmichael/ACESS/ Emisson-data_main.html. The latest figures show that the emission estimates for China have decreased significantly from the 1995 values: from 25.2 to 20.8 million tons (Mt) for SO_2, from 12 to 9.2 Mt for NO_x, and from 115 to 84.1 Mt for CO. The reduction in the estimated SO_2 and NO_x emission is largely attributed to the decreasing industrial coal consumption and the mining of high-quality coal, whereas the decrease of the CO estimate is mainly a result of adopting updated emission factors (D. G. Streets, personal communications, 2001). Table 3 gives the emission ratios derived from the 2000 inventory for Zhejiang (where the present measurements were made), several neighboring provinces, and the Shanghai municipality. Among them, Jiangsu and Shanghai are more industrially developed than Zhejiang, Jiangxi, and Fujian. Table 3 also shows the emission ratios inferred from the winter/nighttime measurements. We have used the concentration ratios to represent the emission ratios of SO_2 to NO_x since their background levels are both near zero. The averaged SO_2 to NO_y^* ratio for the nighttime/winter data set is 1.37 ppbv/ppbv. This value is slightly larger than the emission-derived ratio (1.12 ppbv/ppbv) for Zhejiang but is within the range of 0.96–2.08 for the adjacent provinces.

[23] A large discrepancy is found for the CO to NO_y ratio. The experimentally derived ratio ($\Delta[CO]/\Delta[NO_y^*] = 36$ ppbv/ppbv) is more than 3 times the emission-based value for Zhejiang ($CO/NO_x = 11$ ppbv/ppbv) and is also considerably larger than those for the rest of the provinces and Shanghai. We further compared the observed ratio with those derived for the four quadrants in five grid boxes centered at the study site (with the grid size ranging 0.5° to 10°). This exercise yields a similar result: the observed CO to NO_y^* ratio is more than three times those estimated for all

the quadrants in these boxes. This analysis suggests that the current inventory has significantly underestimated CO emissions from rural areas of China. The lower CO/NO_x ratios in the inventories may be partially explained by the fact that the existing inventories include emissions from the burning of biofuels in cookstoves, but not any open burning such as burning of crop residues and during land clearing (D. G. Streets, personal communication, 2001). Open burning of crop residues is known to produce very high CO/NO_y ratios. We once collected an air sample at an open field burning site near the measurement site and found that the sample contained 3862 ppbv of CO and 17.4 ppbv of NO_y^*, giving an emission ratio of CO to NO_x larger than 100 ppbv/ppbv. It should be noted, however, that other possible causes of the lower CO/NO_x in the inventories, such as an underestimation of the amount and/or emission factor of CO for biofuels, should also be carefully investigated.

4. Summary and Conclusions

[24] We have analyzed the recently obtained 1-year data set of CO, NO_y^*, and SO_2 from a rural site in the Yangtze Delta in eastern China in an attempt to derive their emission ratios. CO and NO_y^* showed good positive correlations with an overall slope of 36 ppbv/ppbv, which is substantially larger than those ($\approx$10 ppbv/ppbv) found at rural sites in industrialized nations. The highest CO/NO_y^* ratios occurred in September–December 1999 and June 2000. The good correlation between CO and the biomass burning tracer CH_3Cl and the lack of correlation with the industrial tracer C_2Cl_4 suggests that the former is a major source for the elevated CO and possibly for other trace gases as well. The large SO_2/NO_y^* ratio (1.37 ppbv/ppbv) reflects the use of coals containing a relatively high sulfur content. The observed SO_2/NO_y^* is comparable with the latest emission inventories. However, a large discrepancy on the CO/NO_y emission ratio exists between the inventory-derived and the measurement-inferred values. The observed ratio is more than three time the values from the emission estimates. An initial comparison with the results from the PEM-West aircraft studies shows that the values of ethyne/CO and propane/ethane for the present inland site are comparable to the ratios in the fresh Asian continental outflow encountered by the aircraft over the western Pacific.

[25] Our study suggests potentially strong emissions of chemically active trace gases (and aerosols) in rural areas of eastern China. The atmospheric and health implications of the rural emissions shall be investigated in greater detail. With regard to ozone pollution, the rural areas alone could emit substantial amounts of ozone precursors (CO, NMHCs, and NO_x) that lead to regional-scale ozone pollution, which could pose a serious health threat to the rural inhabitants. The high levels of regional ozone and ozone precursors could make it even more challenging to control ozone pollution in major urban areas of China. Further studies are needed to improve the estimates and projections of the rapidly changing emissions in China and to look into the potential impacts of rural emissions from Asia on the regional and global environment.

References

Blake, N. J., D. R. Blake, B. C. Sive, T-Y. Chen, F. S. Rowland, J. E. Collins, Jr., G. W. Sachse, and B. E. Anderson, Biomass burning emissions and vertical distribution of atmospheric methyl halides and other reduced carbon gases in the South Atlantic Region, *J. Geophys. Res.*, *101*, 24,141–24,164, 1996.

Blake, N. J., D. R. Blake, T.-Y. Chen, J. E. Collins, Jr., C. W. Sachse, B. E. Anderson, and F. S. Rowland, Distribution and seasonality of selected hydrocarbons and halocarbons over the western Pacific basin during PEM-West A and PEM-West B, *J. Geophys. Res.*, *102*, 28,315–28,331, 1997.

Buhr, M. P., et al., Evaluation of ozone precursor source types using principal component analysis of ambient air measurements in rural Alabama, *J. Geophys. Res.*, *100*, 22,853–22,860, 1995.

Chameides, W. L., et al., Is ozone pollution affecting crop yields in China, *Geophys. Res. Lett.*, *26*, 867–870, 1999a.

Chameides, W. L., et al., Case study of the effects of atmospheric aerosols and regional haze on agriculture: An opportunity to enhance crop yields in China through emission controls?, *Proc. Natl. Acad. Sci.*, *26*, 13,626–13,633, 1999b.

Colbeck, I., and M. Harrison, The concentrations of species of specific C_2–C_6 hydrocarbons in the air of NW England, *Atmos. Environ.*, *10*, 1899–1904, 1985.

Elliott, S., D. R. Blake, R. A. Ruce, C. A. Lai, I. McCreary, L. A. McNair, F. S. Rowland, and A. G. Russell, Motorization of China implies changes in Pacific air chemistry and primary production, *Geophys Res. Lett.*, *24*, 2671–2674, 1997.

Galloway, J. N., Atmospheric acidification: Projections for the future, *Ambio*, *18*, 161–166, 1989.

Hoell, J. M., D. D. Davis, S. C. Liu, R. Newell, M. Shipham, H. Akimoto, R. J. McNeal, R. J. Bendura, and J. W. Drewry, Pacific Exploratory Mission-West A (PEM-West A): September–October 1991, *J. Geophys. Res.*, *101*, 1641–1653, 1996.

Hoell, J. M., D. D. Davis, S. C. Liu, R. Newell, H. Akimoto, R. J. McNeal, and R. J. Bendura, Pacific Exploratory Mission-West B (PEM-West B): February–March 1994, *J. Geophys. Res.*, *102*, 28,223–28,239, 1997.

Hov, O., N. Schmidbauer, and M. Oehme, C_2–C_5 Hydrocarbons in rural South Norway, *Atmos. Environ., Part A*, *25*(9), 1981–1999, 1991.

Kato, N., and H. Akimoto, Anthropogenic emissions of SO_2 and NO_x in Asia: Emission inventories, *Atmos. Environ.*, *26*, 2997–3017, 1994.

Kok, G. L., J. A. Lind, and M. Fang, An airborne study of air quality around the Hong Kong territory, *J. Geophys. Res.*, *102*, 19,043–19,057, 1997.

Lobert, J. M., D. H. Scharffe, W-M. Hao, T. A. Kahlbusch, R. Seuwen, P. Warneck, and P. J. Crutzen, Experimental evaluation of biomass burning emissions: Nitrogen and carbon containing compounds, in *Global Biomass Burning—Atmospheric, Climatic, and Biospheric Implications*, edited by J. S. Levine, pp. 289–304, MIT Press, Cambridge, Mass., 1991.

Luke, W. T., Evaluation of a commercial pulsed flurescence detector, *J. Geophys. Res.*, *102*, 16,255–16,265, 1997.

Luo, C., J. C. St. John, X. J. Zhou, K. S. Lam, T. Wang, and W. L. Chameides, A nonurban ozone air pollution episode over eastern China: Observation and model simulations, *J. Geophys. Res.*, *105*, 1889–1908, 2000.

Neuman, J. A., L. G. Huey, T. B. Ryerson, and D. W. Fahey, Study of inlet materials for sampling atmospheric nitric acid, *Environ. Sci. Technol.*, *33*, 1133–1136, 1999.

Parrish, D. D., M. Trainer, M. P. Buhr, B. A. Watkins, and F. C. Fehsenfeld, Carbon monoxide concentrations and their relation to concentrations of total reactive oxidized nitrogen at two rural U. S. sites, *J. Geophys. Res.*, *96*, 9309–9320, 1991.

Parrish, D. D., et al., The total reactive oxidized nitrogen levels and their partitioning between the individual species at six rural sites in eastern North America, *J. Geophys. Res.*, *98*, 2927–2939, 1993.

Peng, Y., C. Luo, X. Xu, R. Xiang, G. Ding, J. Tang, M. Wang, and X. Yu, The study of distribution character of O_3, NO_x, and SO_2 at rural areas in China, *Q. J. Appl. Meteorol.*, *8*(1), 53–60, 1997.

Streets, D. G., and S. T. Waldhoff, Biofuel use in Asia and acidifying emissions, *Energy*, *23*(12), 1029–1042, 1998.

Streets, D. G., and S. T. Waldhoff, Present and future emissions of air pollutants in China: SO_2, NO_x, and CO, *Atmos. Environ.*, *34*, 363–374, 2000.

Talbot, R. W., et al., Chemical characteristics of continental outflow from Asia to the troposphere over the western Pacific Ocean during February–March 1994: Results from PEM-West B, *J. Geophys. Res.*, *102*, 28,255–28,274, 1997.

Wang, C. J.-L., D. R. Blake, and F. S. Rowland, Seasonal variations in the atmospheric distribution of a reactive chorine compound, tetrachloraethene ($CCl_2 = CCl_2$), *Geophys Res. Lett.*, *22*, 1097–1110, 1995.

Wang, T., K. S. Lam, L. Y. Chan, and A. S. Y. Lee, Trace gas measurements in coastal Hong Kong During the PEM-WEST (B), *J. Geophys. Res.*, *102*, 28,575–28,588, 1997.

Wang, T., T. F. Cheung, M. Anson, and Y. S. Li, Ozone and related gaseous pollutants in the boundary layer of eastern China: Overview of the recent measurements at a rural site, *Geophys Res. Lett.*, *28*, 2373–2376, 2001a.

Wang, T., T. F. Cheung, K. S. Lam, G. L. Kok, and J. M. Harris, The characteristics of ozone and related compounds in the boundary layer of the South China coast: Temporal and vertical variations during autumn season, *Atmos. Environ.*, *35*, 2735–2746, 2001b.

Wang, W. X., and T. Wang, On the origin and the trend of acid rain precipitation in China, *Water Air Soil Pollut.*, *85*, 2295–2300, 1995.

Warneck, P., Chemistry of the Natural Atmosphere, 757 pp., Academic, San Diego, Calif., 1988.

———————————

D. R. Blake, Department of Chemistry, University of California, Irvine, CA 92697, USA.

T. F. Cheung, Y. S. Li, and T. Wang, Department of Civil and Structural Engineering, The Hong Kong Polytechnic University, Hong Kong. (cetwang@polyu.edu.hk)

X. M. Yu, Linan Baseline Air Pollution Monitoring Station, Zhejiang, China.